ELSEVIER

Analytica Chimica Acta 409 (2000) 247–255

ANALYTICA CHIMICA ACTA

www.elsevier.com/locate/aca

Electrochemical and conformational studies of microcystin–LR

F. Yan, M. Ozsoz[1],O.A. Sadik *

Department of Chemistry, State University of New York at Binghamton, PO Box 6016, Binghamton, NY 13902, USA

Received 18 August 1999; accepted 17 November 1999

Abstract

The detection of microcystins in freshwater and in biological samples has become increasingly important due to their toxicity and tumor-promoting nature. This paper describes the electrochemical characterization of microcystin–LR using cyclic voltammetry and anodic stripping voltammetry at different substrates of gold, platinum, glassy carbon and carbon pastes electrodes. Results of electrochemical oxidation reactions indicated that gold-catalyzed complexes were formed between mercury ions and microcystin at approximately 450 mV versus a silver/silver chloride reference electrode. The resulting complex, that was also observed using copper, zinc, lead and gallium ions, was strongly dependent on the concentration of microcystins at picomolar levels with quantitation range of 10 pM–1 nM. The energetics of interaction of the metal ions with the cyclic peptide was studied using semi-empirical molecular orbital calculations. Stable conformation was obtained when the metal ions were localized within the cavity region of the microcystin. This is likely to provide a new approach to the possible mechanisms of detoxification for this class of hepatotoxic peptides. It is also likely to result in the development of suitable electrochemical method of detection for other types of microcystin. ©2000 Elsevier Science B.V. All rights reserved.

Keywords: Microcystins; Electrochemistry; Molecular modeling; Mechanism; Toxicity; Complexation

1. Introduction

Microcystins are a family of low molecular weight, toxic peptides produced by different species of cyanobacteria usually found in lakes, water reservoirs, and recreational facilities [1–5]. Their basic structure is a cyclic heptapeptide and their variations give rise to more than 50 types of microcystins currently known [2,3]. The most extensively studied type is microcystin–LR, which accounts for about 90% of the total toxicity. Microcystins (MCs) and related polypeptides are strong hepatotoxins in fish, birds, and mammals. An acute poisoning by these compounds can result in rapid disorganization of the hepatic architecture [4–8]. Also, microcystins are potent *inhibitors* of protein phosphatases 1 and 2A otherwise known as PP1 and PP2A, respectively [9–11]. PP1 and PP2A are regulatory enzymes present in the cytosol of mammalian cells. The inhibition of these enzymes may provide possible explanation of microcystins as cancer promoters and the formation of primary liver cancer in humans exposed to long-term doses of these toxins through drinking water [12–16]. However, it has not been easy to precisely determine the amount of MCs in water because their concentrations are extremely low and the toxins are confined within complicated

* Corresponding author. Tel.: +1-607-777-4132; fax: +1-607-777-4478.
E-mail address: osadik@binghamton.edu (O.A. Sadik).
[1] Permanent address: Ege University, Faculty of Pharmacy, Bornova, Izmir, Turkey.

0003-2670/00/$ – see front matter ©2000 Elsevier Science B.V. All rights reserved.
PII: S0003-2670(99)00888-0

matrices. The amount of MCs in eutrophic lakes has been estimated to be about 1–2 μg/l [1,3].

The conventional method of analysis of MCs involves freezing the cells, followed by solvent extraction and finally concentrating the toxins by absorption in C_{18} cartridges [17–20]. The toxins are then purified using reverse-phase, high performance liquid chromatography [19,20]. High performance thin-layer chromatography has also been used for purification of cyanobacterial toxins [19]. However, these methods are not suitable for the continuous and intermittent analysis of microcystins. Recently, the identification and quantitation of cyanobacterial toxins were conducted using a mouse bioassay, which has obvious shortcomings, including the need for large numbers of animals [20,21]. Although verifying the presence of toxin still has to be done through the bioassay, other sensitive and specific assays have been developed, including chemical, cytotoxic, and immunological methods.

In addition, the immunoassay for peptide toxin of *Microcystis aeruginosa* has been developed using polyclonal antisera raised in a rabbit [22]. The antisera used were highly specific, producing little cross-reactivity with peptides from *Oscillatoria or Anabaena*. While these methodologies provided screening of less than 1 μg of peptide or alkaloid toxin, a relationship between stereotype and pathogenicity has not been proven. The need for the development of rapid, simple, and low-cost toxicity screening procedures for continuous monitoring and control of pollution has been identified [23,24]. Electrochemical methods provide a quick approach to the detection of MCs due to their simplicity, low costs and suitability for field applications.

In this paper, we report the electrochemical characterization of MCs using CVs and anodic stripping voltammetry. Electrochemical methods have been less frequently reported [25,26]. We investigated the feasibility of binding MC with mercury, lead, cadmium, copper and zinc at the gold electrode. The use of mercury was strongly favored due to its readily accessible electrochemistry as well as its generally favorable uptake at gold electrodes. In addition, mercury can easily be determined using a conventional electrochemical stripping approach. This provides the opportunity to assess the possible binding mechanism of microcystins with metals. In our opinion, this is one of the first instances in which the fundamental electrochemical study of MCs with mercury has been reported. The conformational studies of MC–LR using molecular dynamic calculations provided a means of evaluating the relative stability of the stereotype with metals. This may provide a possible detoxificatiom mechanism for microcystins.

2. Experimental

2.1. Reagents

All solutions were made up in Nanopure, deionized distilled water (17.5 MΩ/cm). Microcystin–LR and RR were obtained from Sigma (St. Louis, MO). Mercuric nitrate, lead, copper and zinc stock solutions were purchased from Fisher Scientific. These were diluted as required for the preparation of standards. Phosphate buffer solution prepared from analytical grade reagents was used as the supporting electrolyte (50 mM, pH 7.0).

2.2. Instrumentation

The electrochemical instrumentation used in these experiments consisted of an EG&G Potentiostat/Galvanostat (Model 263A). Data collection and analysis were conducted using ELECTROCHEMISTRY SOFTWARE Model 270. Electrochemical experiments were conducted using a three-electrode cell with a BAS gold electrode as the working electrode (0.0201 cm^2). Potentials were measured relative to an aqueous, saturated Ag/AgCl double junction (reference electrode) and a platinum wire (auxiliary electrode). Molecular modeling calculations were carried out using the INSIGHT II program from Molecular Simulations.

2.3. Procedures

Cyclic voltammetry experiments were carried out in a 10 ml electrochemical cell using different substrates including gold, glassy carbon, platinum, and carbon paste electrodes. A phosphates buffer was used as the supporting electrolyte (pH 7.0). In anodic stripping voltammetry, mercury film and target metal were

deposited on gold electrodes using a solution containing 100 mg/l mercuric nitrate in 0.1 M HCl at a potential of −0.6 V for 2 min. After deposition, the stripping step was performed with differential pulse voltammetry within potential range of 0.3–0.8 V and at a scan rate of 20 mV/s. The electrode was cleaned at a potential of 1.0 V for 5 min in-between measurements. Microcystins were injected and the solution was stirred for 5 min before repeating the above procedure.

3. Results and discussion

3.1. Cyclic voltammetry

The electrochemical oxidation of aromatic amino acids, tyrosine and related bioactive compounds has been widely reported [27,28]. The structure of MCs and its derivatives showed the presence of oxidizable amino acids, tyrosine (e.g. microcyctin–YR, LR and RR), and arginine (Fig. 1). This suggests that cyclic peptide MCs containing oxidizable tyrosine and non-oxidizable arginine functional groups may be available for derivatization and hence electrochemical characterization. Recently, some workers reported the electrochemical detection of MCs using high performance liquid chromatography [25]. The authors reported the presence of a rather featureless voltammogram for MCs with no CV data shown. Other workers reported the interaction of MCs with copper and Zn at environmentally relevant pH values, and also estimated the strength of binding in relation to the formation constant using polarographic method [26]. In our case, we investigated the cyclic voltammetry of MCs alone as well as in the presence of different electrochemically active species that could act as mediators. These include ferrocene, ruthenium tris (2,2′-bipyridine), potassium ferricyanide and methylene blue. Typical voltammogram recorded for microcystin–LR (MC–LR) is shown in Fig. 2.

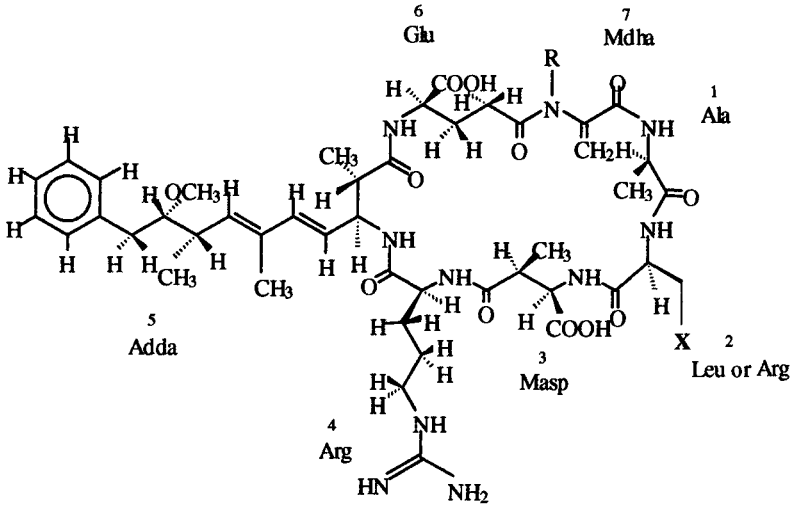

Microcystin – LR	$R = CH_3$, $X = CH(CH_3)_2$
Microcystin – YR	$R = CH_3$, $X = C_6H_4$-p-OH
Microcystin – RR	$R = CH_3$, $X = CH_2CH_2NHC(=NH)NH_2$
Desmethyl-7-microcystin LR	$R = H$, $X = CH(CH_3)_2$

Fig. 1. Structures of microcystin–LR and microcystin–RR.

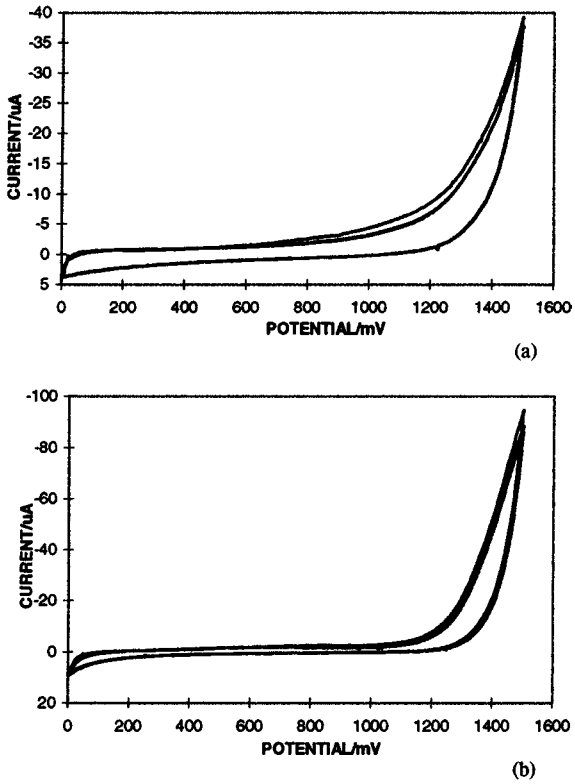

Fig. 2. Cyclic voltammograms recorded for 10 nM MC–LR at (a) glassy carbon, (b) platinum electrodes. Scan rate: 50 mV/s; electrolyte, 50 mM phosphate buffer (pH 7.0).

Results obtained in all these cases indicated that no distinct oxidation peak could be observed for microcystins. These suggest that a slow or irreversible charge transfer reaction has occurred. Hence, for an electrochemical detection method to be developed for the microcystins, the peptide residues would have to be derivatized using an electrochemical label, or an indirect detection method developed. We choose the latter alternative.

3.2. Anodic stripping voltammetry

Microcystins have a spatial structure suitable for binding metallic ions. Amino, carboxyl, nitrogen and oxygen groups within the MC molecule are potentially available for characteristic coordination bonding with metallic ions [29]. Such bond formation can be accompanied by the displacement of protons. The number

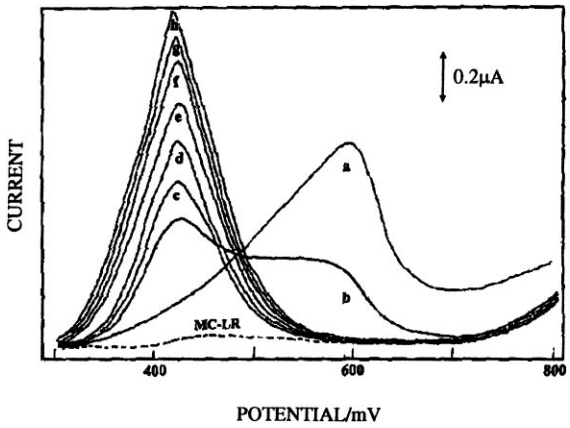

Fig. 3. Differential pulse stripping voltammograms for MC–LR and 5 μM Hg^{2+} at a gold electrode. (a) Mercury ion alone; (b–h) addition of 20 pM increments of MC–LR. Conditions: Deposition potential: −0.6 V; deposition time, 2 min; Differential pulse height: 25 mV, pulse width: 50 mV, scan increment: 2 mV; scan rate: 20 mV/s. The intensity of the metal oxidation peak increased upon the addition of MC–LR; this may suggest a catalytic effect by binding of the microcystin.

of molecules of the ligand will depend on the coordination number of the metal and also on the number of complexing groups in the ligand molecule. The ligands may also function by enveloping the metal ion in a two- or three-dimensional cavity to form stable, solution phase complexes with species that possess similar ionic radius and electropositivity.

Therefore we investigated the simultaneous anodic stripping voltammetry of a solution of MCs and mercury ions. The experiments were carried out at an Au working electrode in a 10-ml electrochemical cell versus the Ag/AgCl reference. The solution contained 5 μM $Hg(NO_3)_2$ in a 0.05 M phosphate buffer at pH 7. Microcystin–LR was used to study possible binding of Hg^{2+} after the voltammetry of mercury at the gold electrode. Results obtained are shown in Fig. 3. It was found that when only MC–LR was present, no oxidation peak was recorded at the gold electrode. This further confirmed our previous CV data, thus indicating that MC–LR is not intrinsically electroactive. However, in the absence of microcystin–LR, we observed the oxidation of free Hg^{2+} at ca.570 mV. When 20 pM of MC–LR was added, an extra peak was obtained at ca. 420 mV, hence leading to a simultaneous decrease in the Hg^{2+} peak. Increasing the concentration

of microcystin–LR in the solution (20 pM additions) caused the Hg^{2+} oxidation peak to shift, thus resulting in a increase in intensity. This is indicative of the binding of Hg^{2+} by microcystin–LR. We believe that the change in the voltammetry of Hg^{2+} observed in Fig. 3 was due to the binding by the microcystin.

Therefore, a possible electrochemical mechanism of the oxidation of the complexed mercury ions is as follows:

$$Hg^{0} \xrightarrow{+0.600} Hg_2^{2+} \xrightarrow{+0.723} Hg^{2} \qquad +0.654 \tag{1}$$

$$Hg^{2+} + MC \xrightarrow{0.450V} \text{Hg-MC complex} \tag{2}$$

Eq. (1) indicates the formal oxidation potentials for mercury involving free cations, including the potentials for the corresponding ionic complexes. The mercury oxidation, either from Hg^0 or Hg^{2+}, occurs at potentials below 0.8 V. The oxidation of gold generally requires higher potentials (above 1.49 V vs. Ag/AgCl). The additional peak obtained at +0.450 V can be attributed to the binding of mercury to microcystin, and this is strongly dependent on the concentration of microcystin (Eq. (2)). Other metals exhibiting comparable, effective ionic radii, stoichiometry and binding constants as Hg^{2+} should be able to display similar characteristics. These include Ag^{+}, Pb^{2+}, Cd^{2+}, and Ga^{3+} [30].The reactions of different metal ions were studied at gold electrodes including zinc, copper, lead, and alkaline earth metals. Fig. 4 is the differential pulse stripping voltammogram recorded for copper ions at the gold electrode. Well-defined anodic stripping voltammograms were also recorded for Zn^{2+}, Cu^{2+}, Cd^{2+}, and Pb^{2+}. Broad anodic currents were obtained for Ga^{3+} and as predicted, no signals were recorded for the alkali and alkaline earth metals including sodium, calcium and magnesium ions. In the case of Zn and Cu, the oxidation peaks were significantly reduced in the presence of varying concentrations of MC–LR. Detection limits recorded for MC–LR were 0.5, 1.0 and 2.0 pM using Zn, Cu, and Hg, respectively. The main parameters of typical calibration lines obtained during the determination of MC–LR using differential pulsed stripping voltammetry are summarized in Table 1. In all these cases, remarkable sensitivity (in the low pM range) was recorded. The linear range was between 10 pM–1 nM with a correlation coefficient of 0.980 or higher.

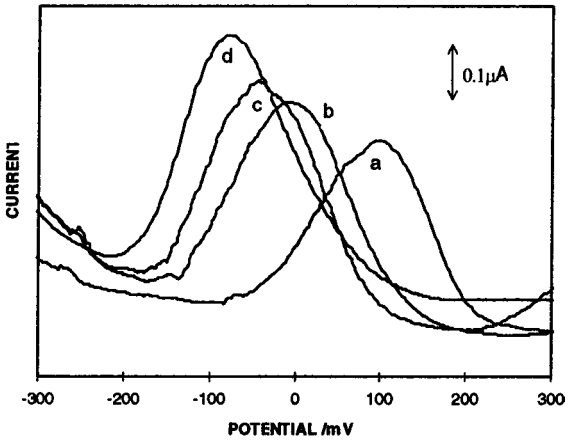

Fig. 4. Differential pulse stripping voltammograms for MC–LR and 5 μM Cu^{2+} at gold electrode. (a) Copper ion alone; (b–e) addition of 10 pM increments of MC–LR. Other conditions as in Fig. 3.

This suggests that a useful analytical method may be developed.

3.3. Mechanism of metal–microcystin complex

Deprotonation of an amide nitrogen in aqueous media in the absence of metal ions requires a very strong basic condition (p*K*a∼15). However, the coordination of the transition metal ions helps to increase the acidity of the amide nitrogen through stabilization of the deprotonated form [31]. The magnitude of this effect depends on the metal ion, and it is remarkable when a five-membered ring chelate is formed [32]. The major forms of Cu(II)–microcystin complexes (Cu(II)–MC) in solution can be described by the equilibria involving the deprotonation of the amide NHs.

$$CuMC \rightleftharpoons Cu(H_{-1}MC) + H^{-1}$$

$$K_1^{H} = \frac{[CuMC]}{[Cu(H_{-1}MC][H^{+}]} \tag{3}$$

$$Cu(H_{-1}MC) \rightleftharpoons Cu(H_{-2}MC) + H^{-1}$$

$$K_2^{H} = \frac{[Cu(H_{-1}MC)]}{[Cu(H_{-2}MC)][H^{+}]} \tag{4}$$

$$Cu(H_{-2}MC) \rightleftharpoons Cu(H_{-3}MC) + H^{-1}$$

$$K_3^{H} = \frac{[Cu(H_{-2}MC)]}{[CuH_{-3}MC][H^{+}]} \tag{5}$$

Table 1
Summary of quantitative detection of MC–LR using differential pulse voltammetry

Metal ion	Binding Constant	Detection limit (pM)	Linear range	ΔE (mV)	Slope	Intercept (nA)	Regression coefficient
Pb^{2+}	9.53±0.37	1.0	10 pM–1.0 nM	−49.9	0.0928	386.2	0.9968
Cd^{2+}	7.79±0.92	2.0	20 pM–600 pM	−8.10	0.0004	2300.8	0.9798
Cu^{2+}	7.94±1.20	1.0	10 pM–1 nM	−200.2	1.5763	491.4	0.9884
Hg^{2+}	10.66±0.23	2.0	10 pM–1 nM	−190.6	0.2321	312.5	0.9877
Zn^{2+}	10.89±0.54	0.5	1 pM–1 nM	−19.6	0.1917	−3229.5	0.9839

The presence of amino nitrogen, carboxyl, and oxygen groups in MCs can encourage strong binding with the metal, which is greatly influenced by the charge. Stability constants were determined and the results indicated that the binding reaction was of intermediate range ($K \approx 10^{10}$) as well as pH-dependent (Table 1). Therefore, the mechanism proposed, which is pH-dependent for the reduction of the complexed ions, is given below:

$$\mathrm{MC} + ne + m\mathrm{Hg}^{2+} \rightarrow \mathrm{Hg(MC)} + \mathrm{HmMC}(E'_{\mathrm{p}}) \quad (6)$$

$$E'_{\mathrm{pc}} = E_{\mathrm{p}} \pm \frac{\mathrm{RT}}{nF} \ln K_{\mathrm{a}} \pm \frac{\mathrm{RT}}{nF} m\mathrm{pH} \quad (7)$$

where E_{pc} is the shift in peak potential after complexing with the metal, E_{p} is the peak potential without MC, n is the number of electrons transferred and m is the protons involved in the reduction. The value of the slope E_{p} from Eq. (6) will enable the determination of the ratio between the number of protons involved and the number of electrons transferred. It appears that microcystin functions as a ligand by enveloping metal ion in a two- or three-dimensional cavity to form a stable solution phase complex. This complex can be measured through a change in the redox state of the metal as depicted in Fig. 5. One strategy for understanding the mechanism of metal–microcystin binding involves the determination of the distribution and speciation of functional groups in the cavity. Using conformational analysis, the functional groups or recognition elements can be identified in a core structure or template.

3.4. Conformational analysis

Using computational techniques, we attempted to calculate the intermolecular forces between the metal ions and the microcystin ligands. Although there is numerous literature available regarding the nature of the toxicity and the mechanisms of action of microcystis peptides, however, their three-dimensional structures were reported only recently. The crystal structure of protein phosphatase-1 complexed with MC–LR has been determined [33]. The structure of MC–LR was obtained from Brookhaven Protein Databank. The atomic charges were calculated using Gasteigner and Hunkel method. The structure of MC–LR was then minimized using semi-empirical molecular orbital package (MOPAC). The evaluation of intermolecular energy was carried out using INSIGHT II (Molecular Simulations). This software program was used to search for the minimal configuration of the metal ion binding to MC–LR. Docking was conducted by placing the metal ion in a configuration particularly appropriate for interaction with the ligand. In addition, docking allowed real-time approximation of the intermolecular energy of the system.

The energy output was obtained in terms of the van der Waals (vdw) and electrostatic energies using

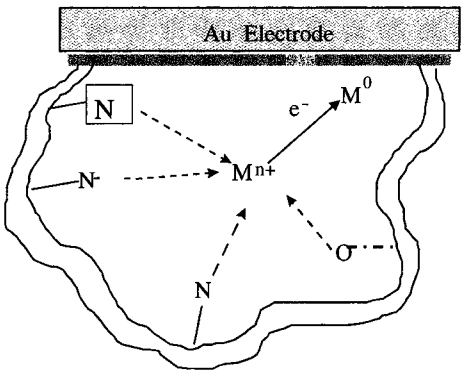

Fig. 5. Schematic of the mechanism of microcystins with metals ions. Conformation of microcystin changes as it wraps itself around the metal ion forming a metal-ion complex at the gold electrodes.

Table 2
Intermolecular energy evaluation of metal–microcystin complex[a]

Residue	van der Waals energy (kcals/mol)	Electrostatic energy (kcals/mol)	Total energy (kcals/mol)
Adda	94021.9	2632.76	96654.7
Glu	232107	2283.13	234390
Mdha	2552.71	4855.49	7408.2
Ala	149736	5788.28	155524
Masp	35921.3	2017.03	37938.4
Leu	7.36137×10^{7}	1957.68	7.36157×10^{7}
Arg	10642.7	1788.01	12430.7
Cavity	163.527	2572.95	2736.48

[a] Adda=3-amino-9-methoxy-2,6,8-trimethyl-10-phenyldeca-4,6-dienoic acid; Masp=D-erythro-β-methylaspartic acid; Mdha=*N*-Methyldehydroalanine, Arg=arginine, Lue=leucine, Ala=Alanine, Glu=Glutamine. [INSIGHT II Modeling Environment, December 1998, San Diego: Molecular Simulations, 1998.].

structure minimization (Table 2). The greatest energy changes were associated with the vdw forces. These include non-bonding energies, which tend to be poorly defined in crystallographic data. Some workers suggested that the stereochemistry of the adda residues was essential for the activity and toxicity of microcystin [34]. Fig. 6 shows the superposition of the average structures of MC–LR with metal ions. The minimum energy configuration of the metal ion binding to MC–LR was located to be in the cavity region

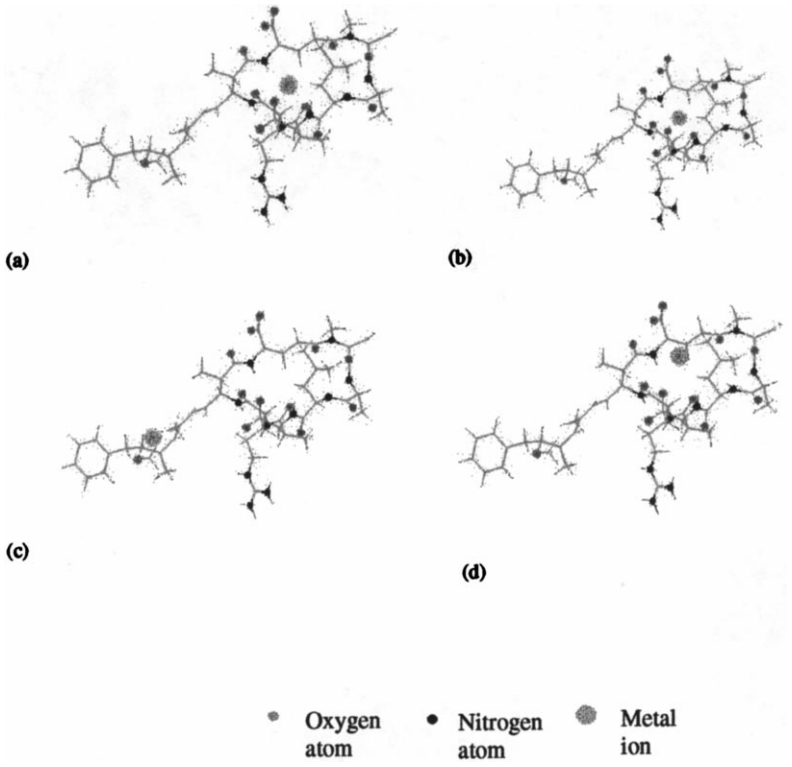

Fig. 6. Minimum energy configuration of metal–microcystin LR complex. The intermolecular energy minimization with the metal ion was evaluated interactively while one structure is moved relative to the other. Metal ion binding in (a) cavity region, (b) masp residue, (c) adda residue, (d) glu residue.

(Table 2). The largest differences between these structures can be seen in the segment containing mdha[7] and leu[2]. The conformational differences between the backbones in this region can be attributed to changes in the total energy. It was interesting to note that the relatively stable conformation was obtained when the metal ion was localized in the cavity region (Table 2). This confirmed the mechanism depicted in Fig. 5. In our opinion, this can provide a possible detoxification mechanism for microcystins and related cyclic peptides including okadaic acids. We are currently working on isolating these intermediates as well as studying the solution phase reaction using microcystins.

4. Conclusions

The electrochemical characterization and conformational studies of microcystin–LR have been carried out. Results indicated that the toxin possesses no intrinsic electrochemical activity. However, the toxin binds to metals such as zinc, copper and mercury. Its reaction with mercury at the gold electrode resulted in a complex at approximately 0.450 V versus silver/silver chloride reference electrode. This work suggests that microcystins could act as a ligand for the formation of a stable complex with mercury at approximately 0.450 V. This complex, which was also recorded using cadmium, lead, copper, gallium and zinc ions, was not observed at other conducting substrates such as platinum, glassy carbon and carbon paste electrodes. This suggested that gold might be acting as a catalyst during the formation of the microcystin–mercury complex. The complex formed was strongly dependent on the concentration of microcystins at picomolar levels and linear range obtained with mercury was between 10 pM–1.0 nM with a correlation coefficient of 0.9877. We propose that the mechanism by which these cyclic peptides interact with the metals involved a deprotonation of the peptide and a simultaneous reduction of the metal ion. Conformational analysis indicates that the most stable form of MC–LR binding with the metal ion was obtained when the metal was located in the cavity region. Consequently, this may provide a new approach for the electrochemical detection of MCs and the possible detoxification mechanisms.

References

[1] W. Carmichael, in: Watanabe, Harada, Carmichael, Fujiki (Eds.), Toxic Microcystis, CRC Press, FL, Chap. 1, 1996.
[2] H. Utkilen, in: Synthetic Prokaryotes, N. Mann, N. Carr (Eds.), Plenum Press, New York, Chap. 7, pp. 221–231, 1992.
[3] I.R. Falconer, A. Jackson, J. Langley, M.T.C. Runnegar, Aust. J. Biol. Sci. 34 (1981) 179.
[4] W. Carmichael, United States Environmental Protection Agency, 1600/R-92/079, 1992, p.32.
[5] R. Matsushima, S. Yushizawa, M. Watanabe, K. Harada, M. Furusawa, W. Carmichael, H. Fujiki, Biochem. Biophy. Res. Commun. 171 (1990) 867.
[6] S.B. Hooser, M. Kuhlenschmidlt, A. Dahlem, U. Beasley, W. Carmichael, Toxicon 29 (1991) 589.
[7] J. Erickson, D. Toivola, J. Meriluoto, H. Haraki, Y. Han, D. Hartshorne, Biochem. Biophys. Res. Commun. 173 (1990) 1347.
[8] S. Yoshizawa, R. Matsushima, M. Watanabe, K. Harada, A. Ichihara, W.W. Carmichael, H. Fujku, J. Cancer Res. Clin. Oncol. 116 (1990) 609.
[9] R. Honkanener, J. Zwiller, R. Moore, S. Daily, B.S. Khatra, M. Dukelow, A.L. Boynton, J. Biol. Chem. 265 (1990) 19401.
[10] C. Mackintosh, K. Beattie, S. Klumpp, P. Cohen, G. Codd, FEBS Lett. 264 (1990) 187.
[11] R. Nishiwaki-Matsushima, S. Ohta, S. Nishiwaki, M. Suganuma, K. Kohyama, T. Ishiwaka, W.W. Carmichael, H. Fujiki, J. Cancer Res. Clin. Oncol. 118 (1992) 420.
[12] I. Falconer, Environ. Toxic Water Quality 6 (1991) 177.
[13] W. Carmichael, Sci. Am. 1 (1994) 64.
[14] S. Yu, in: Z.Y. Tang, M.C. Wu, S.S. Xia, (Eds.), Primary Liver Cancer, China Academic Publishers/Springer, Berlin, 1989, pp.1–137.
[15] Y. Ueno, S. Nagata, T. Tsutsumi, A. Hasegawa, M.F. Watanabe, H.D. Park, G.C. Chen, G. Chen, S.Z. Yu, Carcinogenesis 17 (1996) 1317.
[16] A. Zaporozee, Groundwater 17 (1979) 1999.
[17] L. Lawton, G.E. Edward, G.A. Codd, Analyst 119 (1994) 1525.
[18] Y. Tanaka, S. Takenaka, H. Matsuo, S. Kitamori, H. Tokiwa, Toxicol. Environ. Chem. 39 (1993) 21.
[19] C. Edwards, L.A. Lawton, K.A. Beattie, G.A. Codd, S. Pleasante, G. Dear, Rapid Commun. Mass Spectrom. 7 (1993) 714.
[20] T. Sano, K. Nohara, F. Shirai, K. Kaya, Int. J. Environ. Anal. Chem. 49 (1992) 163.
[21] D. Rawson, J. Willmer, Toxicity Assessment 2 (1987) 325.
[22] C. Rivassea, P. Racaud, A. Deguin, M-C. Henion, Environ. Sci. Technol. 33 (1999) 1520.
[23] O.A. Sadik, J. Van Emon, ChemTech 27 (6) (1997) 38.
[24] O.A. Sadik, J. Van Emon, Biosensor & Bioelectronics 11 (8) (1996) 1.
[25] J. Meriluoto, B. Kincaid, M. Smyth, M. Wasberg, J. Chromatogr. A. 810 (1998) 226.
[26] A. Humble, M. Geogrey, G. Codd, Water Res. 31 (7) (1997) 1679.
[27] R. Dawson, J. Steves, F. Lorden, S. Oparil, Peptides 6 (1985) 1173.

[28] M. Hawley, S. Tatawawadi, S. Piekarski, R.N. Adams, J. Am. Chem. Soc. 89 (1967) 447.
[29] R.H. Crist, K. Oberholser, M. Nguyen, J. Am Chem. Soc. 15 (1981) 1212.
[30] J.A. Dean, Lange's Handbook of Chemistry 4.5, McGraw-Hill, New York, 1992.
[31] H. Sigel, R.B. Martin, Chem. Rev. 82 (1982) 385.
[32] M.K. Kim, A.E. Martell, J. Am. Chem. Soc. 88 (1966) 914.
[33] J. Goldberg, H. Huang, Y. Kwon, P. Greengard, A.G. Nain, J. Kuriyan, Nature 376 (1995) 745.
[34] K. Harada, K. Ogawa, K. Matsura, H. Murata, M. Suzuki, M. Watanabe, Y. Itzeno, N. Nakayama, Chem. Res. Toxicol. 3 (1990) 473.